JOURNAL OF THERMOPHYSICS AND HEAT TRANSFER
Vol. 27, No. 1, January–March 2013

Hydromagnetic Hiemenz Slip Flow of Convective Micropolar Fluid Towards a Stretching Plate

Mostafa A. A. Mahmoud* and Shimaa E. Waheed†
Benha University, Banha 13518, Egypt

DOI: 10.2514/1.T4016

This paper is concerned with the effect of slip velocity on the steady two-dimensional flow of a micropolar fluid near a stagnation point at a stretching plate in the presence of a uniform transverse magnetic field and thermal radiation with the bottom surface of the plate is heated by convection from a hot fluid. The governing system of partial differential equations describing the problem is converted into a system of nonlinear ordinary differential equations using similarity transformation, and then solved numerically using the Chebyshev spectral method. Numerical results for the velocity, microrotation, and temperature are shown graphically and discussed for various values of different parameters. Moreover, the numerical values of the local skin-friction coefficient and the local Nusselt number for these parameters are also tabulated and discussed.

I. Introduction

MICROPOLAR fluids are those with a microstructure belonging to a class of fluids with nonsymmetrical stress tensor. The theory of micropolar fluids, first proposed by Eringen [1], who is capable of describing such fluids, and later [2] generalized the micropolar-fluid theory to include the thermal effects. This theory is expected to provide a mathematical model for non-Newtonian fluid behavior, which can be used to analyze the behavior of exotic lubricants, liquid crystals, polymeric fluids, colloidal fluids, real fluids with suspensions, and animal blood. Extensive reviews of this theory and its applications can be found in the review articles by Ariman et al. [3,4], and the books by Lukaszewicz [5] and Eringen [6]. Several researchers have studied the boundary-layer flow and heat transfer on a moving surface with and without a magnetic field under different boundary conditions [7–11].

For some industrial applications such as glass production and furnace design, nuclear-power plants, gas turbines, and in space-technology applications such as cosmical flight aerodynamic rocket-propulsion systems, plasma physics, and spacecraft-reentry aerothermodynamics that operate at higher temperature, radiation effects can be quite significant. In view of this, the effects of radiation on the flow and heat transfer of a micropolar fluid past a continuously moving plate have been studied by many authors [12–17].

Stagnation-point flow has attracted many investigations during the past several decades because of its wide applications in many practical problems like cooling of electronic devices by fans, cooling of nuclear reactors, and many hydrodynamic processes. Hiemenz [18] was the first one who studied the two-dimensional (2-D) flow of fluid near a stagnation point. This problem was extended numerically by Schlichting and Bussman [19], and analytically by Ariel [20] to include the effect of suction. Peddieson and McNitt [21] derived the boundary-layer equations for a 2-D micropolar flow at a stagnation point on a stationary wall. The stagnation-point flows toward a surface that is stretched have been considered, for example, by Nazar et al. [22] and recently by Ishak et al. [23]. Ramadan and Al-Nimr [24] numerically studied the impulsively started convection in planar and axisymmetric stagnation-point flow.

In the aforementioned studies, the effect of slip condition has not been taken into consideration, while the study of magnetomicropolar fluid flows in the slip-flow regimes with heat transfer has important engineering applications, such as in power generators, refrigeration coils, transmission lines, electric transformers, and heating elements. From the kinetic theory of gases of slightly rarefied flows, the no-slip boundary condition is replaced by a slip boundary condition, and for a prescribed surface temperature, a thermal-jump condition will occur [25]. Kiwan and Al-Nimr studied the effects of velocity slip and temperature-jump condition on 1) the convection heat transfer induced by a stretching flat plate [26], and 2) stagnation-point flow toward a stationary flat plate [27]. There is no kinetic theory for surface heat-flux boundary condition or convective surface heat-flux boundary condition, or liquid fluids or non-Newtonian fluids. Therefore, calculations for heat transfer at the microscale assume that there is no thermal jump comparing the velocity jump. If this is correct, then for surface heat fluxes, liquids, and non-Newtonian fluids, the temperature boundary condition at the wall will be the same as for nonslip flows. The previous researchers have assumed that there is a nonjump temperature [28–36].

Except for a few, the stagnation-point flows of a micropolar fluid have been studied using either a constant surface temperature or a constant heat-flux boundary condition. Very recently, the study of heat-transfer problem for the boundary layer concerning a convective boundary condition has received considerable attention because of its use in several engineering and industrial processes, such as transpiration-cooling process, material drying, laser-pulse heating, etc. Aziz [37] presented a similarity solution for laminar boundary layer over a flat plate with a convective boundary condition. Abraham and Sparrow [38] investigated the validity of the relative model for the problem of laminar fluid flow, which results from the simultaneous motion of a freestream and its bounding surface in the same direction. Sparrow and Abraham [39] developed a method for determining universal solutions for streamwise variation of the temperature of a moving sheet in the presence of an independently moving fluid. Ishak et al. [40] have studied the radiation effects within the thermal boundary over a moving plate under a convective boundary condition. Jafar et al. [41] studied the steady laminar 2-D stagnation-point flow and heat transfer of an incompressible viscous fluid impinging normal to a horizontal plate, with the bottom surface of the plate heated by convection from a hot fluid. Bataller [42] has presented the effects of radiation on Blasius and Sakiadis flows with convective boundary condition. Also, Makinde and Aziz [43] and Yao et al. [44] have investigated boundary-layer flows over a vertical plate and stretching/shrinking sheet, respectively, under the same convective boundary conditions. Motivated by the aforementioned investigations and applications, in this paper, the authors investigate a heat-transfer problem with a convective boundary condition for the

Received 15 August 2012; revision received 16 October 2012; accepted for publication 17 October 2012; published online 10 January 2013.

*Department of Mathematics, Faculty of Science; mostafabdelhameed@yahoo.com.

†Department of Mathematics, Faculty of Science; currently Taif Univesity, Taif, KSA; shimaa_ezat@yahoo.com.

2-D flow of a micropolar fluid near a stagnation point at a stretching plate in the presence of thermal radiation with slip velocity.

II. Formulation of the Problem

The equations governing the behavior of an incompressible steady micropolar fluid in vectorial form [1,2] are the 1) conservation of mass [Eq. (1)], 2) conservation of linear momentum [Eq. (2)], 3) conservation of angular momentum [Eq. (3)], and 4) the energy [Eq. (4)].

$$\nabla \cdot \underline{U} = 0 \tag{1}$$

$$\rho(\underline{U} \cdot \nabla)\underline{U} = -\nabla p + (\mu + k)\nabla^2 \underline{U} + k\nabla \times \underline{\sigma} + \rho \underline{F} \tag{2}$$

$$\rho J(\underline{U} \cdot \nabla)\underline{\sigma} = (\alpha^* + \beta^* + \gamma^*)\nabla(\nabla \cdot \underline{\sigma}) - \gamma\nabla \times (\nabla \times \underline{\sigma}) + k\nabla \times \underline{U} - 2k\underline{\sigma} + \rho \underline{l} \tag{3}$$

$$\rho c_p(\underline{U} \cdot \nabla)T = \kappa_f \nabla^2 T - \nabla q_r + \varphi + Q \tag{4}$$

in which $\underline{F}$ is the body force per unit mass; $\underline{l}$ is the body couple per unit mass; $\underline{U}$ is the translation vector; $\underline{\sigma}$ is the microrotation vector; p is the pressure; α^*, β^*, γ^* and k are the material constants for micropolar fluids; ρ is the fluid density; J is the microinertia; μ is the dynamic viscosity; and κ_f is the thermal conductivity. T is the fluid temperature, φ is the dissipation function, Q is used to present the internal heat generation density caused by joule heating and the chemical or nuclear reaction, q_r is the radiation heat-flux vector, and c_p is the specific heat at constant pressure. Consider the steady, incompressible 2-D laminar stagnation-point flow of an electrically conducting radiating micropolar fluid over a stretching plate, which coincides with the plane $y = 0$. The flow is generated as the consequence of linear stretching of the boundary sheet, caused by the simultaneous application of equal and opposite forces along the x axis while keeping the origin fixed. The flow being in the region $y > 0$ is shown in Fig. 1. A uniform magnetic field of strength B_0 is imposed along the y axis. The magnetic Reynolds number of the flow is taken to be small enough so that the induced magnetic field is assumed to be a negligible field in comparison with the applied magnetic field. The plate is considered to be electrically nonconducting. The stretching-surface velocity is assumed to vary linearly with x (i.e., $u_w = ax$). The freestream is moving with velocity $U = bx$ and at a constant temperature T_∞, in which a and b are positive constants, and x measures the distance from the stagnation point. Whereas, the upper boundary of the surface is maintained at a constant temperature T_w. It was assumed that all physical properties of the fluid are fixed.

Under usual boundary-layer and Boussinesq approximations, the governing boundary-layer equations taking into account the presence of the radiation effect are given by the following equations [45,46]:

$$\frac{\partial u}{\partial x} + \frac{\partial v}{\partial y} = 0 \tag{5}$$

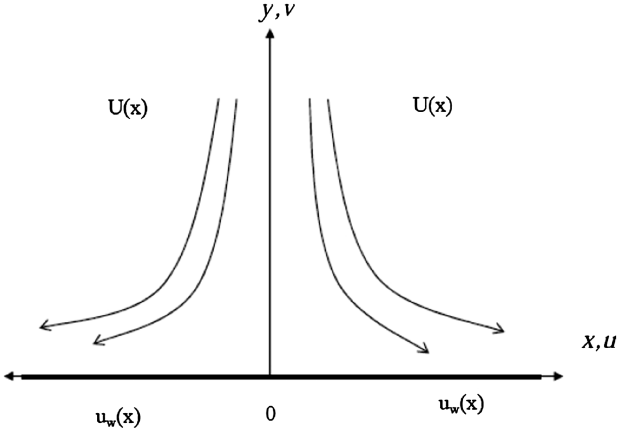

Fig. 1 Flow model and coordinate system.

$$u\frac{\partial u}{\partial x} + v\frac{\partial u}{\partial y} = U\frac{dU}{dx} + \left(\nu + \frac{k}{\rho}\right)\frac{\partial^2 u}{\partial y^2} + \frac{k}{\rho}\frac{\partial N}{\partial y} - \frac{\sigma B_0^2}{\rho}(u - U) \tag{6}$$

$$u\frac{\partial N}{\partial x} + v\frac{\partial N}{\partial y} = \frac{\gamma_0}{\rho j}\frac{\partial^2 N}{\partial y^2} - \frac{k}{\rho j}\left(2N + \frac{\partial u}{\partial y}\right) \tag{7}$$

$$u\frac{\partial T}{\partial x} + v\frac{\partial T}{\partial y} = \frac{\kappa}{\rho c_p}\frac{\partial^2 T}{\partial y^2} - \frac{1}{\rho c_p}\frac{\partial q_r}{\partial y} \tag{8}$$

in which u and v are the velocity components in the x and y directions, respectively. T is the fluid temperature, N is the component of the microrotation vector normal to the xy plane, μ is the dynamic viscosity of the fluid, k is the gyro-viscosity, ρ is the density of the fluid, σ is the electrical conductivity, κ is the thermal conductivity, c_p is the specific heat at constant pressure, q_r is the radiative heat flux, and γ_0 is the spin-gradient viscosity.

The authors of the current study follow the recent work of the author [22] by assuming that γ_0 is given by

$$\gamma_0 = (\mu + k/2)j = \mu(1 + K/2)j \tag{9}$$

This equation gives a relation between the coefficient of viscosity and microinertia, in which $K = k/\mu(> 0)$ is the material parameter, $j = \nu/a$, $\sqrt{j}$ is the reference length, and $\nu = \mu/\rho$ is the kinematic viscosity. This assumption is invoked to allow the field equations to predict the correct behavior in the limiting case when the microstructure effects become negligible and the total spin N is reduced to the angular velocity [47].

The boundary conditions for the flowfield are

$$\begin{aligned} u &= ax + \alpha^*\left[(\mu + k)\frac{\partial u}{\partial y} + kN\right] \\ v &= 0, \qquad N = -m_0\frac{\partial u}{\partial y}, \quad \text{at } y = 0 \\ u &\to U, \qquad N \to 0, \quad \text{as } y \to \infty \end{aligned} \tag{10}$$

in which α^* is the slip coefficient, and m_0 $(0 \le m_0 \le 1)$ is the boundary parameter. When the boundary parameter $m_0 = 0$, $N = 0$ is obtained, which is the no-spin condition, that is, the microelements in a concentrated particle flow close to the wall are not able to rotate (as stipulated by Jena and Mathur [48]). The case $m_0 = 1/2$ represents the weak concentration of microelements. The case corresponding to $m_0 = 1$ is used for the modeling of turbulent boundary-layer flow (see Peddieson and McNitt [21]).

It is also assumed the bottom surface of the plate is to be heated by convection from a hot fluid at uniform temperature T_f, which provides a heat-transfer coefficient h_f. Here, $T_f > T_w > T_\infty$. Then, the boundary conditions at the plate surface and far into the cold fluid can be expressed as [42]:

$$-\kappa\left(\frac{\partial T}{\partial y}\right)_w = h_f[T_f - T_w] \quad \text{at } y = 0 \quad T \to T_\infty, \quad \text{as } y \to \infty \tag{11}$$

Using the Rosseland approximation [15]

$$q_r = (-4\sigma^*/3k^*)\frac{\partial T^4}{\partial y} \tag{12}$$

in which σ^* is the Stefan–Boltzmann constant, and k^* is the mean absorption coefficient. Assuming that the temperature differences within the flow are sufficiently small such that T^4 may be expressed as a linear function of temperature. The fluid is considered to be gray, absorbing–emitting radiation, but a nonscattering medium and the Rosseland approximation are used to describe the radiative heat flux in the energy equation. The radiative heat flux in the x direction is

considered negligible in comparison to the y direction. Hence, expanding T^4 in the Taylor series about T_∞ and neglecting higher terms to give

$$T^4 \cong 4T_\infty^3 T - 3T_\infty^4 \tag{13}$$

in which the higher-order terms of the expansion are neglected.

The following dimensionless variables are introduced:

$$\eta = \left(\frac{a}{\nu}\right)^{1/2} y, \qquad N = ax\left(\frac{a}{\nu}\right)^{1/2} h(\eta)$$
$$u = axf'(\eta), \qquad v = -(a\nu)^{1/2} f$$
$$\theta(\eta) = \frac{T - T_\infty}{T_f - T_\infty} \tag{14}$$

Because of Eq. (14), the continuity equation [Eq. (5)] is automatically satisfied, and Eqs. (6–9) will give then

$$(1+K)f''' + ff'' - f'^2 + Kh' + \lambda^2 + M(\lambda - f') = 0 \tag{15}$$

$$\left(1 + \frac{K}{2}\right)h'' + fh' - f'h - K(2h + f'') = 0 \tag{16}$$

$$(1+R)\theta'' + Prf\theta' = 0 \tag{17}$$

The transformed boundary conditions are then given by

$$f' = 1 + \alpha[1 + K(1-m_0)]f'' \qquad f = 0, \qquad h = -m_0 f'',$$
$$\theta' = -\beta(1-\theta), \quad \text{at } \eta = 0 \qquad f' \to \lambda, \qquad h \to 0,$$
$$\theta \to 0, \quad \text{as } \eta \to \infty \tag{18}$$

in which primes denote differentiation with respect to η, $M = \sigma B_0^2/a\rho$ is the permeability parameter, $\lambda = b/a$ is the velocity-ratio parameter, $\alpha = \alpha^* \mu\sqrt{a/\nu}$ is the slip parameter, $Pr = \mu c_p/\kappa$ is the Prandtl number, $R = (16\sigma^* T_\infty^3)/(3k^*\kappa)$ is the radiation parameter, and $\beta = (-h_f/\kappa)(\nu/a)^{\frac{1}{2}}$ is the surface-convection parameter.

The physical quantities of interest are the local skin-friction coefficient C_{f_x} and the local Nusselt number N_{u_x}, which are defined, respectively, as

$$C_{f_x} = -\frac{2\tau_w}{\rho(ax)^2} \qquad Nu_x = \frac{xq_w}{\kappa(T_f - T_\infty)} \tag{19}$$

in which the wall shear stress τ_w and the heat transfer from the plate q_w are defined by

$$\tau_w = \left[(\mu + k)\frac{\partial u}{\partial y} + kN\right]_{y=0} \qquad q_w = -\left[\kappa\frac{\partial T}{\partial y}\right]_{y=0} \tag{20}$$

Using the similarity variables [Eq. (14)], the following equation is obtained:

$$\frac{1}{2}C_{f_x}Re_x^{1/2} = -[1 + K(1-m_0)]f''(0) \qquad Nu_x Re_x^{-1/2} = -\theta'(0) \tag{21}$$

in which $R_{e_x} = (u_w x/\nu)$ is the local Reynolds number.

III. Method of Solution

The domain of the governing boundary-layer equations [Eqs. (15–18)] is the unbounded region $[0, \infty)$. However, for all practical reasons, this could be replaced by the interval $0 \le \eta \le \eta_\infty$, in which η_∞ is some large number to be specified for computational convenience. Using the algebraic mapping

$$\chi = 2\frac{\eta}{\eta_\infty} - 1$$

the unbounded region $[0, \infty)$ is finally mapped onto the finite domain $[-1, 1]$, and the problem expressed by equations [Eqs. (15–18)] is transformed into

$$(1+K)f'''(\chi) + \left(\frac{\eta_\infty}{2}\right)[f(\chi)f''(\chi) - f'^2(\chi)] + \left(\frac{\eta_\infty}{2}\right)^2[Kh'(\chi) - Mf'(\chi)] + \left(\frac{\eta_\infty}{2}\right)^3(\lambda^2 + M\lambda) = 0 \tag{22}$$

$$\left(1 + \frac{K}{2}\right)h''(\chi) + \left(\frac{\eta_\infty}{2}\right)[f(\chi)h'(\chi) - f'(\chi)h(\chi)] - K\left[2\left(\frac{\eta_\infty}{2}\right)^2 h(\chi) + f''(\chi)\right] = 0 \tag{23}$$

$$(1+R)\theta''(\chi) + \left(\frac{\eta_\infty}{2}\right)Prf(\chi)\theta'(\chi) = 0 \tag{24}$$

The transformed boundary conditions are given by

$$f'(-1) = \left(\frac{\eta_\infty}{2}\right) + \left(\frac{2}{\eta_\infty}\right)\alpha[1 + K(1-m_0)]f''(-1)$$
$$f(-1) = 0, \qquad f'(1) = \left(\frac{\eta_\infty}{2}\right)\lambda$$
$$h(-1) = -m_0\left(\frac{2}{\eta_\infty}\right)^2 f''(-1), \qquad h(1) = 0$$
$$\theta'(-1) = -\beta\left(\frac{\eta_\infty}{2}\right)[1 - \theta(-1)], \qquad \theta(1) = 0 \tag{25}$$

in which, now, differentiation in Eqs. (22–25) will be with respect to the new variable χ.

The technique is accomplished by starting with a Chebyshev approximation for the highest-order derivatives f''', h'', and θ'', and generating approximations to the lower-order derivatives f'', f', f, h', h, θ', and θ as follows:

Setting $f''' = \phi(\chi)$, $h'' = \psi(\chi)$, and $\theta'' = \zeta(\chi)$, then by integration the following equations are obtained:

$$f''(\chi) = \int_{-1}^{\chi} \phi(\chi)\,d\chi + C_1^f \tag{26}$$

$$f'(\chi) = \int_{-1}^{\chi}\int_{-1}^{\chi} \phi(\chi)\,d\chi\,d\chi + C_1^f(\chi + 1) + C_2^f \tag{27}$$

$$f(\chi) = \int_{-1}^{\chi}\int_{-1}^{\chi}\int_{-1}^{\chi} \phi(\chi)\,d\chi\,d\chi\,d\chi + C_1^f\frac{(\chi+1)^2}{2} + C_2^f(\chi + 1) + C_3^f \tag{28}$$

$$h'(\chi) = \int_{-1}^{\chi} \psi(\chi)\,d\chi + C_1^h \tag{29}$$

$$h(\chi) = \int_{-1}^{\chi}\int_{-1}^{\chi} \psi(\chi)\,d\chi\,d\chi + C_1^h(\chi + 1) + C_2^h \tag{30}$$

$$\theta'(\chi) = \int_{-1}^{\chi} \zeta(\chi)\,d\chi + C_1^\theta \tag{31}$$

$$\theta(\chi) = \int_{-1}^{\chi}\int_{-1}^{\chi} \zeta(\chi)\,d\chi\,d\chi + C_1^\theta(\chi + 1) + C_2^\theta \tag{32}$$

From the boundary condition [Eq. (25)], the following equations are obtained:

$$C_1^f = \frac{1}{2+\alpha[1+K(1-m_0)](\frac{2}{\eta_\infty})} \times \left[\left(\frac{\eta_\infty}{2}\right)(\lambda-1) - \int_{-1}^{1}\int_{-1}^{\chi}\phi(\chi)\,\mathrm{d}\chi\,\mathrm{d}\chi\right]$$

$$C_2^f = \left(\frac{\eta_\infty}{2}\right) + \alpha[1+K(1-m_0)]\left(\frac{2}{\eta_\infty}\right)C_1^f$$

$$C_3^f = 0$$

$$C_1^h = -\frac{1}{2}\int_{-1}^{1}\int_{-1}^{\chi}\psi(\chi)\,\mathrm{d}\chi - \frac{1}{2}C_2^h$$

$$C_2^h = -\frac{m_0(\frac{2}{\eta_\infty})(\lambda-1)}{2+\alpha[1+K(1-m_0)](\frac{2}{\eta_\infty})} + \frac{m_0(\frac{2}{\eta_\infty})^2}{2+\alpha[1+K(1-m_0)](\frac{2}{\eta_\infty})}\int_{-1}^{1}\int_{-1}^{\chi}\phi(\chi)\,\mathrm{d}\chi\,\mathrm{d}\chi$$

$$C_1^\theta = -\frac{1}{2}\int_{-1}^{1}\int_{-1}^{\chi}\zeta(\chi)\,\mathrm{d}\chi\,d\chi - \frac{1}{2}C_2^\theta$$

$$C_2^\theta = -\frac{(\frac{2}{\eta_\infty})}{2\beta+(\frac{2}{\eta_\infty})}\int_{-1}^{1}\int_{-1}^{\chi}\zeta(\chi)\,\mathrm{d}\chi\mathrm{d}\chi - \frac{(\frac{2}{\eta_\infty})}{2\beta+(\frac{2}{\eta_\infty})} + 1$$

Therefore, approximations to Eqs. (26–32) can be given as follows:

$$f_i(\chi) = \sum_{j=0}^{n} l_{ij}^f\phi_j + d_i^f, \qquad f_i'(\chi) = \sum_{j=0}^{n} l_{ij}^{f1}\phi_j + d_i^{f1}, \qquad f_i''(\chi) = \sum_{j=0}^{n} l_{ij}^{f2}\phi_j + d_i^{f2} \tag{33}$$

$$h_i(\chi) = \sum_{j=0}^{n} l_{ij}^{\bar{h}}\psi_j + \sum_{j=0}^{n} l_{ij}^{h}\phi_j + d_i^h,$$

$$h_i'(\chi) = \sum_{j=0}^{n} l_{ij}^{\bar{h}1}\psi_j + \sum_{j=0}^{n} l_{ij}^{h1}\phi_j + d_i^{h1} \tag{34}$$

$$\theta_i(\chi) = \sum_{j=0}^{n} l_{ij}^{\theta}\zeta_j + d_i^{\theta}, \qquad \theta_i'(\chi) = \sum_{j=0}^{n} l_{ij}^{\theta1}\zeta_j + d_i^{\theta1} \tag{35}$$

for all $i = 0(1)n$, in which

$$l_{ij}^\theta = b_{ij}^2 - \frac{1}{2\beta+(\frac{2}{\eta_\infty})}\left[\beta(\chi_i+1) + \left(\frac{2}{\eta_\infty}\right)\right]b_{nj}^2,$$

$$d_i^\theta = -\frac{1}{2\beta+(\frac{2}{\eta_\infty})}\left[\beta(\chi_i+1) + \left(\frac{2}{\eta_\infty}\right)\right] + 1$$

$$l_{ij}^{\theta1} = b_{ij} - \frac{\beta}{2\beta+(\frac{2}{\eta_\infty})}b_{nj}^2, \qquad d_i^{\theta1} = -\frac{\beta}{2\beta+(\frac{2}{\eta_\infty})}$$

$$l_{ij}^h = \frac{m_0(\frac{2}{\eta_\infty})^2}{2+\alpha[1+K(1-m_0)](\frac{2}{\eta_\infty})}\left[1-\frac{(\chi_i+1)}{2}\right]b_{nj}^2,$$

$$d_i^h = \frac{m_0(\frac{2}{\eta_\infty})(\lambda-1)}{2+\alpha[1+K(1-m_0)](\frac{2}{\eta_\infty})}\left[\frac{(\chi_i+1)}{2}-1\right]$$

$$l_{ij}^{h1} = -\frac{m_0(\frac{2}{\eta_\infty})^2}{2\{2+\alpha[1+K(1-m_0)]\left(\frac{2}{\eta_\infty}\right)\}}b_{nj}^2,$$

$$d_i^{h1} = \frac{m_0(\frac{2}{\eta_\infty})(\lambda-1)}{2\left\{2+\alpha[1+K(1-m_0)]\left(\frac{2}{\eta_\infty}\right)\right\}}$$

$$l_{ij}^{\bar{h}} = b_{ij}^2 - \frac{(\chi_i+1)}{2}b_{nj}^2, \qquad l_{ij}^{\bar{h}1} = b_{ij} - \frac{1}{2}b_{nj}^2$$

$$l_{ij}^f = b_{ij}^3 - \frac{1}{2+\alpha[1+K(1-m_0)]\left(\frac{2}{\eta_\infty}\right)} \times \left\{\frac{(\chi_i+1)^2}{2} + \alpha[1+K(1-m_0)](\chi_i+1)\left(\frac{2}{\eta_\infty}\right)\right\}b_{nj}^2$$

$$d_i^f = (\chi_i+1)\left(\frac{\eta_\infty}{2}\right) + \frac{(\lambda-1)(\frac{\eta_\infty}{2})}{2+\alpha[1+K(1-m_0)]\left(\frac{2}{\eta_\infty}\right)} \times \left\{\frac{(\chi_i+1)^2}{2} + \alpha[1+K(1-m_0)](\chi_i+1)\left(\frac{2}{\eta_\infty}\right)\right\}$$

$$l_{ij}^{f1} = b_{ij}^2 - \frac{1}{2+\alpha[1+K(1-m_0)]\left(\frac{2}{\eta_\infty}\right)} \times \left\{(\chi_i+1) + \alpha[1+K(1-m_0)]\left(\frac{2}{\eta_\infty}\right)\right\}b_{nj}^2$$

$$d_i^{f1} = \left(\frac{\eta_\infty}{2}\right) + \frac{(\lambda-1)(\frac{\eta_\infty}{2})}{2+\alpha[1+K(1-m_0)]\left(\frac{2}{\eta_\infty}\right)} \times \left\{(\chi_i+1) + \alpha[1+K(1-m_0)]\left(\frac{2}{\eta_\infty}\right)\right\}$$

$$l_{ij}^{f2} = b_{ij} - \frac{1}{2+\alpha[1+K(1-m_0)]\left(\frac{2}{\eta_\infty}\right)}b_{nj}^2,$$

$$d_i^{f2} = \frac{(\lambda-1)(\frac{\eta_\infty}{2})}{2+\alpha[1+K(1-m_0)]\left(\frac{2}{\eta_\infty}\right)}$$

in which

$$b_{ij}^2 = (\chi_i - \chi_j)b_{ij}$$

and b_{ij} are the elements of the matrix B, as given in [49].

By using Eqs. (33–35), one can transform Eqs. (22–24) to the following system of nonlinear equations in the highest derivatives:

$$(1+K)\phi_i + \left(\frac{\eta_\infty}{2}\right)\left[\left(\sum_{j=0}^{n} l_{ij}^f\phi_j + d_i^f\right)\left(\sum_{j=0}^{n} l_{ij}^{f2}\phi_j + d_i^{f2}\right) - \left(\sum_{j=0}^{n} l_{ij}^{f1}\phi_j + d_i^{f1}\right)^2\right] + \left(\frac{\eta_\infty}{2}\right)^2\left[K\left(\sum_{j=0}^{n} l_{ij}^{\bar{h}1}\psi_j + \sum_{j=0}^{n} l_{ij}^{h1}\phi_j + d_i^{h1}\right) - M\left(\sum_{j=0}^{n} l_{ij}^{f1}\phi_j + d_i^{f1}\right)\right] + \left(\frac{\eta_\infty}{2}\right)^3(\lambda^2 + M\lambda) = 0 \tag{36}$$

$$\left(1+\frac{K}{2}\right)\psi_i + \left(\frac{\eta_\infty}{2}\right)\left[\left(\sum_{j=0}^{n} l_{ij}^f\phi_j + d_i^f\right) \times \left(\sum_{j=0}^{n} l_{ij}^{\bar{h}1}\psi_j + \sum_{j=0}^{n} l_{ij}^{h1}\phi_j + d_i^{h1}\right) - \left(\sum_{j=0}^{n} l_{ij}^{f1}\phi_j + d_i^{f1}\right) \times \left(\sum_{j=0}^{n} l_{ij}^{\bar{h}}\psi_j + \sum_{j=0}^{n} l_{ij}^{h}\phi_j + d_i^{h}\right)\right] - K\left[2\left(\frac{\eta_\infty}{2}\right)^2\left(\sum_{j=0}^{n} l_{ij}^{\bar{h}}\psi_j + \sum_{j=0}^{n} l_{ij}^{h}\phi_j + d_i^{h}\right) + \left(\sum_{j=0}^{n} l_{ij}^{f2}\phi_j + d_i^{f2}\right)\right] = 0 \tag{37}$$

$$(1+R)\zeta_i + \left(\frac{\eta_\infty}{2}\right)Pr\left(\sum_{j=0}^{n} l_{ij}^f\phi_j + d_i^f\right)\left(\sum_{j=0}^{n} l_{ij}^{\theta1}\zeta_j + d_i^{\theta1}\right) = 0 \tag{38}$$

This system is then solved using Newton's iteration method.

Table 1 Comparison between the values of $-\theta'(0)$ for various values of λ and Pr with $K = 0$ and $M = 0$ in the absence of R

$Pr\lambda$	Pop et al. [51]			Boutros et al. [50]			Present work		
	0.5	1	1.5	0.5	1	1.5	0.5	1	1.5
0.1	0.381	0.600	0.773	0.3827	0.6051	0.7770	0.3827	0.6025	0.7769
0.2	0.406	0.621	0.793	0.4073	0.6256	0.7972	0.4073	0.6254	0.7972
0.5	0.471	0.689	0.859	0.4728	0.6925	0.8648	0.4727	0.6925	0.8648
1.0	0.562	0.793	0.970	0.5641	0.7979	0.9772	0.5642	0.7979	0.9773
2.0	0.708	0.971	1.168	0.7118	0.9787	1.1781	0.7116	0.9786	1.1782
3.0	0.828	1.122	1.339	0.8335	1.1321	1.352	0.832	1.1299	1.350

Table 2 Comparison between the values of $-f''(0)$ for various values of λ with $K = 0$ and $M = 0$

λ	$-f''(0)$		
	Pop et al. [51]	Boutros et al. [50]	Present work
0.1	0.9694	0.9696	0.96939
0.2	0.9189	0.9182	0.91811
0.5	0.6673	0.66726	0.66726
2.0	−2.0174	−2.0175	−2.0174
3.0	−4.7290	−4.72928	−4.7297

Table 3 Comparison between the numerical results and the results given by Boutros et al. [50] of $-f''(0)$ for various values of λ and M with $K = 0$

$M\lambda$	Boutros et al. [50]			Present work		
	0.5	1.0	1.5	0.5	1.0	1.5
0.1	1.15837	1.32111	1.46612	1.15836	1.32110	1.46612
0.2	1.07683	1.21562	1.34038	1.07683	1.21562	1.34038
0.5	0.75401	0.83212	0.90369	0.75402	0.83212	0.90369
2.0	−2.13632	−2.24910	−2.35667	−2.13632	−2.24910	−2.3566
3.0	−4.9337	−5.13038	−5.31997	−4.9338	−5.13037	−5.31996

IV. Results and Discussion

To assess the accuracy of the present numerical method, the numerical results obtained for $-f''(0)$ and $-\theta'(0)$ are compared with those obtained by Boutros et al. [50] and Pop et al. [51], taking into account that $K = 0$. The results show good agreement as seen in Tables 1–3.

The authors have considered in some detail the influence of the various parameters such as the material parameter K, the magnetic parameter M, the velocity-ratio parameter λ, the slip parameter α, the radiation parameter R, and the surface-convection parameter β on the velocity, microrotation, and temperature profiles, which are shown in Figs. 2–14. The samples of the velocity and microrotation profiles for the different values of the material parameter K when the other parameters are fixed are presented in Figs. 2 and 3, respectively. It is seen from Fig. 2 that for $\lambda > 1$, the dimensionless velocity f' decreases with the increase of K near the surface; the inverse is true away from the surface, and the opposite is true for $\lambda < 1$. The microrotation profiles h increase as K increases for $\lambda > 1$, whereas for $\lambda < 1$, the profiles decrease as K increases near the surface, and the reverse is true at a larger distance from the surface, which is shown in Fig. 3, whereas Fig. 4 presents the effect of the magnetic parameter M on f'. It is noticed that for $\lambda < 1$, f' decreases with the increase of M, whereas f' increases for $\lambda > 1$. Figure 5 displays the influence of M on h. It is obvious that for $\lambda > 1$, h decreases as M increases near the surface; the inverse is true away from the surface, and the opposite is true for $\lambda < 1$. This is because when the imposed pressure force $(\sigma B_0^2/\rho)U$ overcomes the Lorentz force $(\sigma B_0^2/\rho)u$ (i.e., $U > u$), the effect of the magnetic-interaction parameter is to increase the velocity and decrease the microrotation profiles near the plate, and the opposite is true away from the plate. Similarly, when the Lorentz force dominates over the imposed pressure force (i.e., $U < u$),

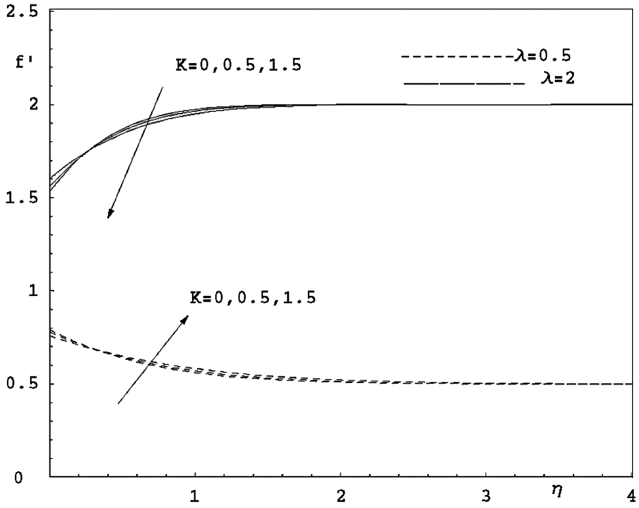

Fig. 2 Velocity profiles for various values of K with $M = 0.5$, $\alpha = 0.5$, $Pr = 0.72$, $\beta = 5$, and $R = 0.3$.

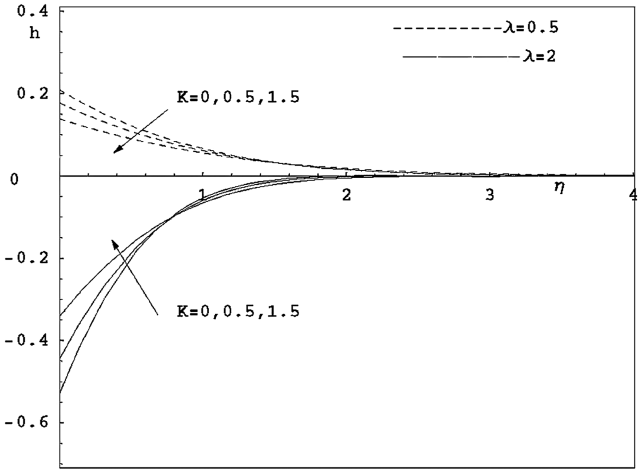

Fig. 3 Microrotation profiles for various values of K with $M = 0.5$, $\alpha = 0.5$, $Pr = 0.72$, $\beta = 5$, and $R = 0.3$.

the effect of the magnetic-interaction parameter will decrease the velocity and increase the microrotation profiles near the plate, and the opposite is true away from the plate. Figure 6 illustrates the effects of M on the temperature profiles θ. It is observed that θ increases with the increase of M for the case $\lambda < 1$, but for $\lambda > 1$, the effects of M are not illustrated. From this figure, it can be seen that the effect of M on θ has no significant effect on the temperature inside the boundary layer. Figure 7 shows the variation of $f'(\eta)$, with η for various values of the slip parameter α. It is seen that for $\lambda > 1$, f' increases with the increase of α, and it decreases with the increase of α for $\lambda < 1$. The microrotation profiles for different values of α have been illustrated in Fig. 8. From this figure, it is noticed that for $\lambda > 1$, h increases with the increase of α, but for $\lambda < 1$, h decreases as α increases. The increase in the value of the slip parameter in the enhancement of the

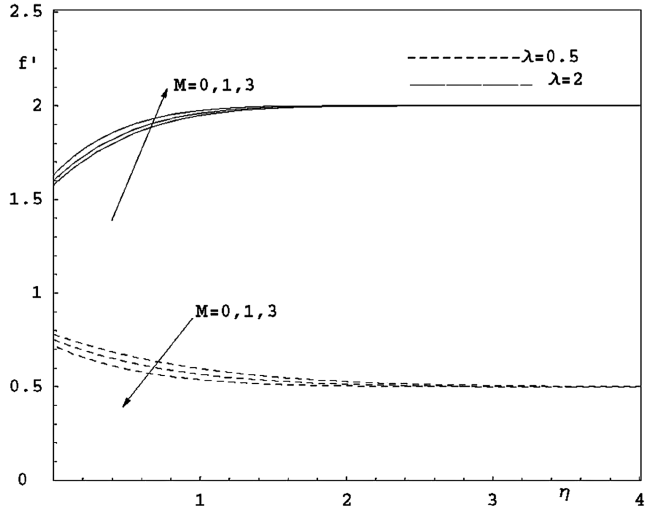

Fig. 4 Velocity profiles for various values of M with $K = 1.2$, $\alpha = 0.5$, $Pr = 0.72$, $\beta = 5$, and $R = 0.3$.

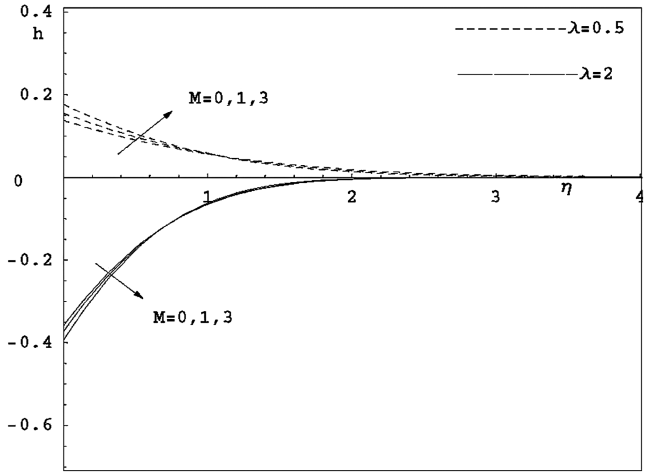

Fig. 5 Microrotation profiles for various values of M with $K = 1.2$, $\alpha = 0.5$, $Pr = 0.72$, $\beta = 5$, and $R = 0.3$.

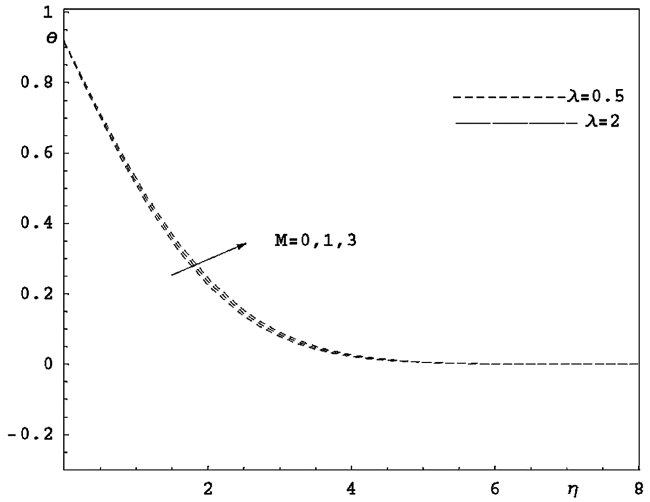

Fig. 6 Temperature profiles for various values of M with $K = 1.2$, $\alpha = 0.5$, $Pr = 0.72$, $\beta = 5$, and $R = 0.3$.

velocity and microrotation profiles inside the boundary layer for $\lambda > 1$ is noticed. The opposite is true for $\lambda < 1$. This behavior is readily understood from the slip-velocity condition at the surface in Eq. (18). Figure 9 shows the effect of α on θ. From this figure, one

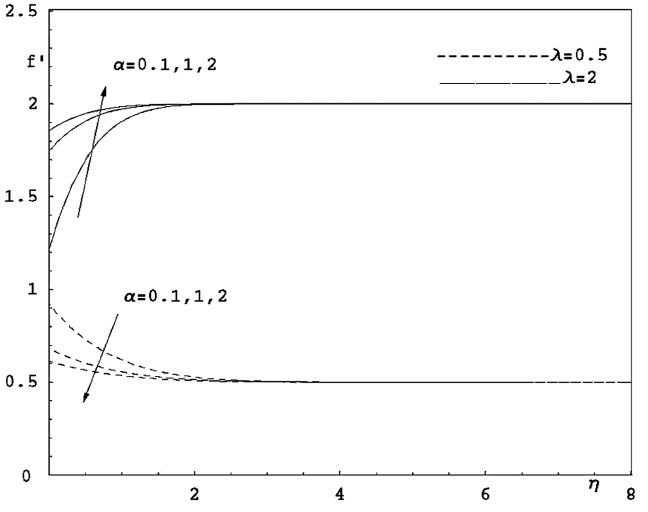

Fig. 7 Velocity profiles for various values of α with $K = 1.2$, $M = 0.5$, $Pr = 0.72$, $\beta = 5$, and $R = 0.3$.

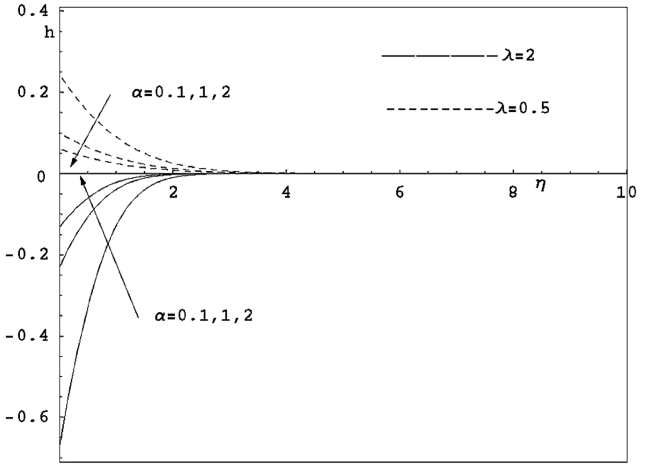

Fig. 8 Microrotation profiles for various values of α with $K = 1.2$, $M = 0.5$, $Pr = 0.72$, $\beta = 5$, and $R = 0.3$.

sees that for $\lambda > 1$, the temperature profiles decrease as α increases, whereas the opposite is true for $\lambda < 1$. The effects of the velocity-ratio parameter λ on f', h, and θ are displayed in Figs. 10–12, respectively. It is seen from Fig. 10 that for $\lambda > 1$, that is, the freestream velocity is greater than the stretching-surface velocity, the boundary-layer thickness increases as λ increases. On the other hand, when $\lambda < 1$, that is, the stretching-surface velocity exceeds the freestream velocity, the boundary-layer thickness decreases with increasing λ. It is noticed that for $\lambda = 1$, that is, the surface of the stretching surface is equal to the freestream velocity, there is no formation of the boundary layer. In Fig. 11, one can see that h decreases on both $\lambda > 1$ and $\lambda < 1$. It is observed from Fig. 12 that θ decreases as λ increases.

From Fig. 13, it is seen that with the increase in the radiation parameter R, the fluid temperature increases for both cases $\lambda > 1$ and $\lambda < 1$. The increase of radiation parameter R implies the release of heat energy from the flow region by means of radiation; this can also be explained by the fact that the effect of radiation is to increase the rate of energy transport to the fluid and, accordingly, increase the fluid temperature. Figure 14 presents the effect of the surface-convection parameter β on θ. It is observed that the plate surface temperature increases as β increases that for both cases of $\lambda > 1$ and $\lambda < 1$. In fact, as $\beta \to \infty$, the solution approaches the classical solution for the constant surface temperature. This can be seen from the boundary condition [Eq. (18)], which reduces to $\theta(0) = 1$ as $\beta \to \infty$.

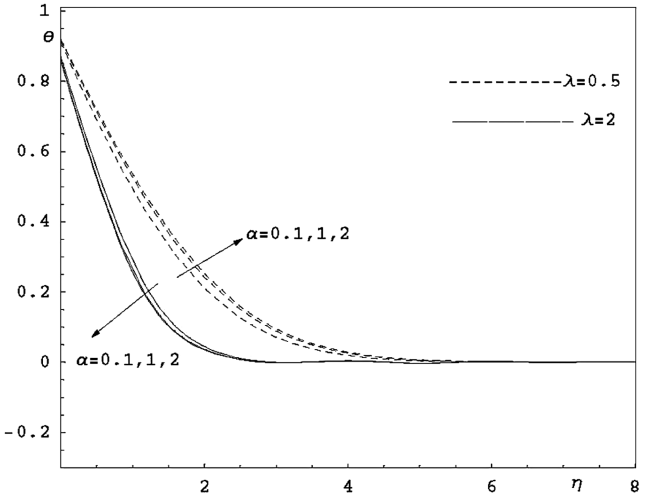

Fig. 9 Temperature profiles for various values of α with $K = 1.2$, $M = 0.5$, $Pr = 0.72$, $\beta = 5$, and $R = 0.3$.

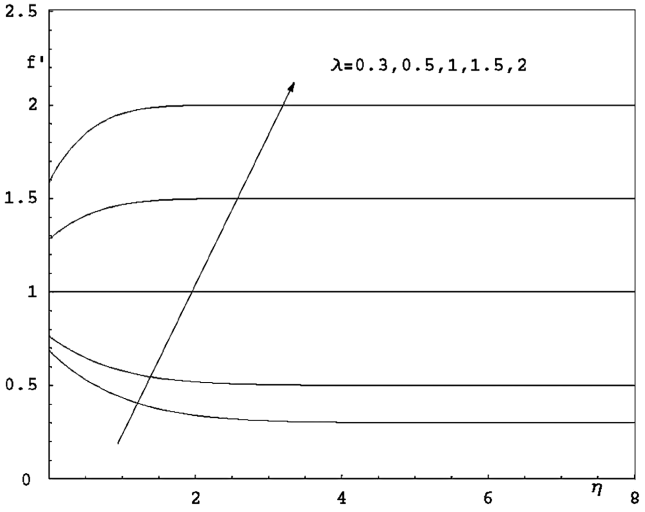

Fig. 10 Velocity profiles for various values of λ with $K = 1.2$, $M = 0.5$, $\alpha = 0.5$, $Pr = 0.72$, $\beta = 5$, and $R = 0.3$.

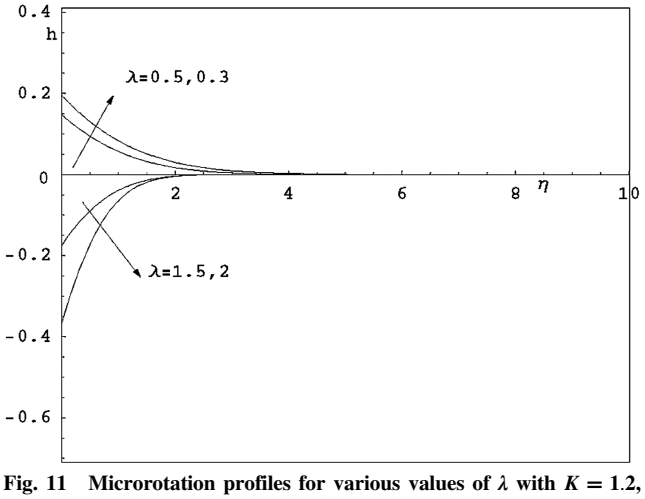

Fig. 11 Microrotation profiles for various values of λ with $K = 1.2$, $M = 0.5$, $\alpha = 0.5$, $Pr = 0.72$, $\beta = 5$, and $R = 0.3$.

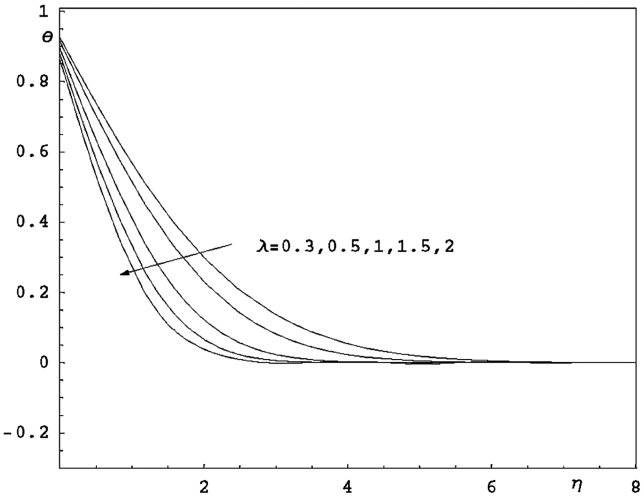

Fig. 12 Temperature profiles for various values of λ with $K = 1.2$, $M = 0.5$, $\alpha = 0.5$, $Pr = 0.72$, $\beta = 5$, and $R = 0.3$.

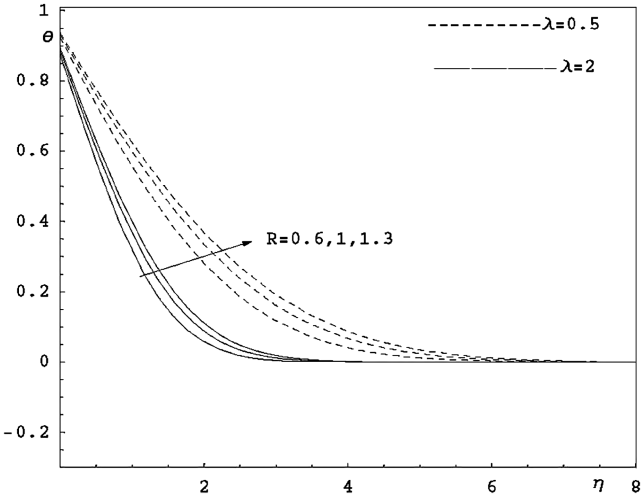

Fig. 13 Temperature profiles for various values of R with $M = 0.5$, $\alpha = 0.5$, $Pr = 0.72$, $\beta = 5$, $K = 1.2$.

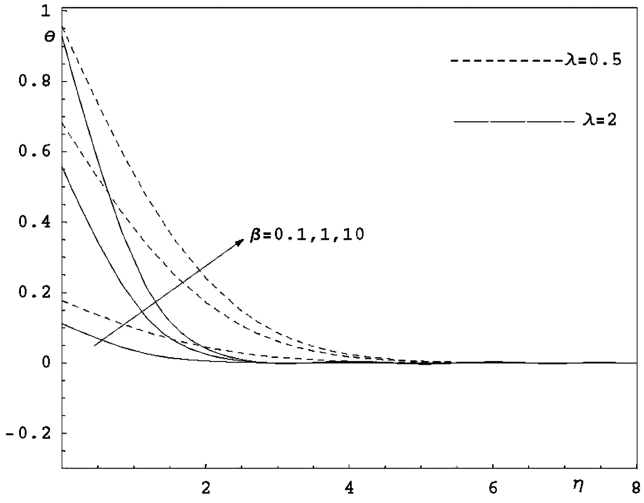

Fig. 14 Temperature profiles for various values of β with $M = 0.5$, $\alpha = 0.5$, $Pr = 0.72$, $R = 0.3$, and $K = 1.2$.

Figures 15–17 illustrate the effects of λ, α, M, K, and β on the local skin-friction coefficient and the local Nusselt number with $\lambda > 1$ and $\lambda < 1$, respectively. From these figures, one observes that for $\lambda > 1$, M has the effect of decreasing the local skin-friction coefficient. The local Nusselt number increases with increasing M for $\lambda > 1\lambda > 1$; the opposite is true for $\lambda < 1$. Moreover, increasing K and α enhances the local skin-friction coefficient for $\lambda > 1$ and reduces it for $\lambda < 1$, whereas the local Nusselt number decreases as K increases for $\lambda > 1$,

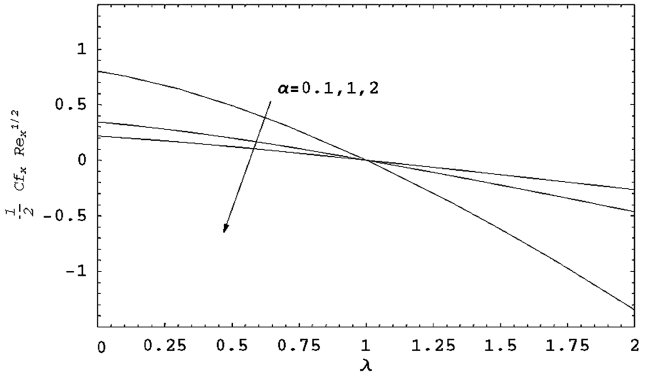

a)

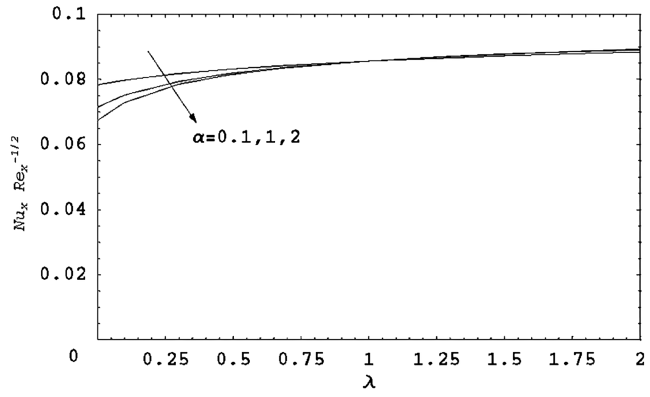

b)

Fig. 15 a) Local skin-friction cofficient and b) local Nusselt number as a function of λ for various values of α.

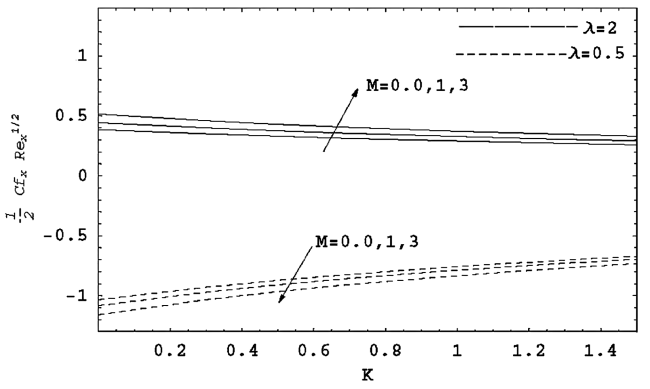

a)

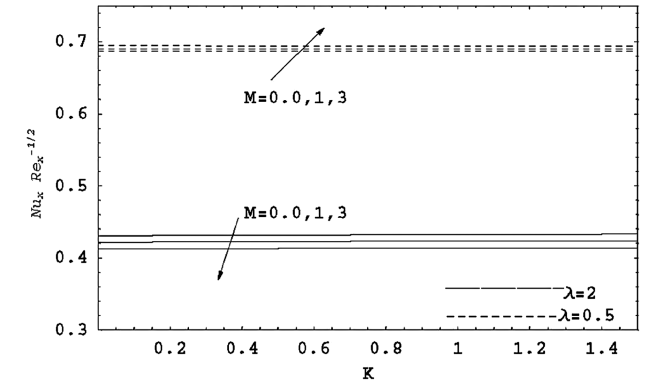

b)

Fig. 16 a) Local skin-friction cofficient and b) local Nusselt number as a function of K for various values of M.

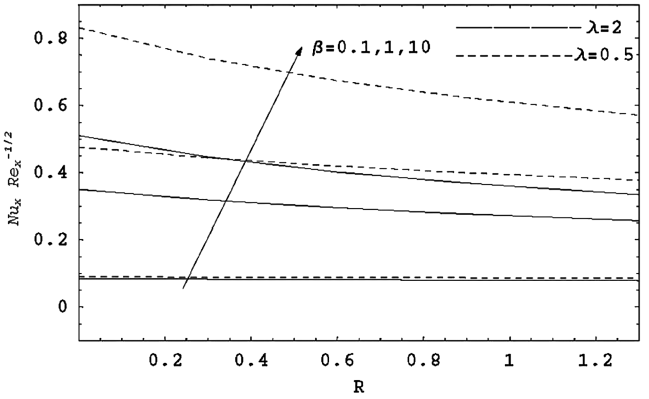

Fig. 17 Local Nusselt number as a function of R for various values of β with $\alpha = 0.5$, $Pr = 0.72$, $M = 0.5$, and $K = 1.2$.

and it increases as K increases for $\lambda < 1$. The inverse is true for α. It is also found that the local skin-friction coefficient decreases with increasing λ, but the local Nusselt number increases as λ increases. Moreover, it is noticed that the values of $f''(0)$ are negative when $\lambda < 1$, which means that the surface exerts a drag force on the fluid, but when $f''(0)$ is positive for $\lambda > 1$, the fluid velocity is enhanced, as clearly seen in Fig. 10. Moreover, the local Nusselt number decreases with the increase of R in both cases for the velocity-ratio parameter λ ($\lambda > 1$ and $\lambda < 1$), but it increases with the increase of β for both cases $\lambda > 1$ and $\lambda < 1$.

V. Conclusions

The problem of steady two-dimensional flow of micropolar fluid near a stagnation point at a stretching plate with radiation taking into account the presence of convective boundary condition and slip velocity has been investigated. Using similarity transformations, the governing equations have been transformed into a system of coupled nonlinear ordinary differential equations, which are solved numerically by using the Chebyshev spectral method. The effects of various parameters M, K, α, λ, R, and β on the flow and heat characteristics were examined. It was found that the local skin-friction coefficient increases as the material parameter and the slip parameter increase, whereas it decreases as the magnetic parameter increases for $\lambda > 1\lambda > 1$; the opposite is true for $\lambda < 1$. It is also found that the local skin-friction coefficient decreases with increasing the velocity-ratio parameter, but the local Nusselt number increases as the velocity-ratio parameter increases. The local Nusselt number decreases as the material parameter increases for $\lambda > 1$, whereas it increases as the material parameter increases for $\lambda < 1$. The inverse is true for the slip parameter and the magnetic parameter. Also, it was found that for both cases $\lambda > 1$ and $\lambda < 1$, the local Nusselt number increases with increasing the surface-convection parameter, whereas the radiation parameter leads to a decrease in the local Nusselt number.

References

[1] Eringen, A. C., "Theory of Micropolar Fluids," *Journal of Mathematics and Mechanics*, Vol. 16, No. 1, 1966, pp. 1–18. doi:10.1512/iumj.1967.16.16001

[2] Eringen, A. C., "Theory of Thermomicropolar Fluids," *Journal of Mathematical Analysis and Applications*, Vol. 38, No. 2, 1972, pp. 480–495. doi:10.1016/0022-247X(72)90106-0

[3] Ariman, T., Turk, M. A., and Sylvester, N. D., "Microcontinuum Fluid Mechanics—A Review," *International Journal of Engineering Science*, Vol. 11, No. 8, 1973, pp. 905–915. doi:10.1016/0020-7225(73)90038-4

[4] Ariman, T., Turk, M. A., and Sylvester, N. D., "Applications of Microcontinuum Fluid Mechanics," *International Journal of Engineering Science*, Vol. 12, No. 4, 1974, pp. 273–279. doi:10.1016/0020-7225(74)90059-7

[5] Lukaszewicz, G., *Micropolar Fluids: Theory and Application*, Birkhäuser, Basel, 1999, pp. 230–233.

[6] Eringen, A. C., *Microcontinuum Field Theories, II: Fluent Media*, Springer, New York, 2001.

[7] Soundalgekar, V. M., and Takhar, H. S., "Flow of Micropolar Fluid Past a Continuously Moving Plate," *International Journal of Engineering Science*, Vol. 21, No. 8, 1983, pp. 961–965. doi:10.1016/0020-7225(83)90072-1

[8] Hady, F. M., "Short Communication on the Solution of Heat Transfer to Micropolar Fluid from a Non-Isothermal Stretching Sheet with Injection," *International Journal of Numerical Methods for Heat & Fluid Flow*, Vol. 6, No. 6, 1996, pp. 99–104. doi:10.1108/09615539610131299

[9] Mahmoud, M. A. A., "Thermal Radiation Effects on MHD Flow of a Micropolar Fluid Over a Stretching Surface with Variable Thermal Conductivity," *Physica A: Statistical Mechanics and Its Applications*, Vol. 375, No. 2, 2007, pp. 401–410. doi:10.1016/j.physa.2006.09.010

[10] Pal, D., and Chatterjee, S., "Heat and Mass Transfer in MHD Non-Darcian Flow of a Micropolar Fluid Over a Stretching Sheet Embedded in a Porous Media with Non-Uniform Heat Source and Thermal Radiation," *Communications in Nonlinear Science and Numerical Simulation*, Vol. 15, No. 7, 2010, pp. 1843–1857. doi:10.1016/j.cnsns.2009.07.024

[11] Mendez, F., and Treviño, C., "Heat Transfer Analysis on a Moving Flat Sheet Emerging into Quiescent Fluid," *Journal of Thermophysics and Heat Transfer*, Vol. 16, No. 3, 2002, pp. 373–378. doi:10.2514/1.6690

[12] Perdikis, C., and Raptis, A., "Heat Transfer of a Micropolar Fluid by the Presence of Radiation," *Heat and Mass Transfer*, Vol. 31, No. 6, 1996, pp. 381–382. doi:10.1007/BF02172582

[13] Kim, Y. J., and Fedorov, A. G., "Transient Mixed Radiative Convection Flow of a Micropolar Fluid Past a Moving, Semi-Infinite Vertical Porous Plate," *International Journal of Heat and Mass Transfer*, Vol. 46, No. 10, 2003, pp. 1751–1758. doi:10.1016/S0017-9310(02)00481-7

[14] Mahmoud, M. A. A., Mahmoud, A. M., and Waheed, S. E., "Hydromagnetic Boundary Layer Micropolar Fluid Flow Over a Stretching Surface Embedded in a Non-Darcian Porous Medium with Radiation," *Mathematical Problems in Engineering*, Vol. 2006, No. 39392, 2006, pp. 1–10, Article ID 39392.

[15] Raptis, A., "Radiation and Free Convection Flow Through a Porous Medium," *International Communications in Heat and Mass Transfer*, Vol. 25, No. 2, 1998, pp. 289–295. doi:10.1016/S0735-1933(98)00016-5

[16] Ishak, A., Nazar, R., and Pop, I., "Boundary-Layer Flow of a Micropolar Fluid on a Continuous Moving or Fixed Surface," *Canadian Journal of Physics*, Vol. 84, No. 5, 2006, pp. 399–410. doi:10.1139/p06-059

[17] Chen, T. M., "Radiation Effects on the Magnethydrodynamic Free Convection Flow," *Journal of Thermophysics and Heat Transfer*, Vol. 22, No. 1, 2002, pp. 125–128. doi:10.2514/1.32202

[18] Hiemenz, K., "Die Grenzschicht an Einem in den Gleichförmigen Flüssigkeitsstrom Eingetauchten Geraden Kreiszylinder," *Dingler's Polytechnic Journal*, Vol. 326, No. 21, 1911, pp. 321–410.

[19] Schlichting, H., and Bussmann, K., "Exakte Lösungen für die laminare Grenzschicht mit Absaugung und Ausblasen," *Schriften der Deutschen Akademie der Luftfahrtforschung, 7B, Nr. 2*, edited by Schlichting, H., and Gersten, K., "Boundary-Layer Theory," Pt. I, 8th ed., Springer-Verlag, New York, 2000, pp. 302–303.

[20] Ariel, P. D., "Stagnation Point Flow with Suction: An Approximate Solution," *Journal of Applied Mechanics*, Vol. 61, No. 4, 1994, pp. 976–978. doi:10.1115/1.2901589

[21] Peddieson, J. Jr., and McNitt, R. P., "Boundary-Layer Theory for a Micropolar Fluid," *Recent Advances in Engineering Science*, edited by Eringen, A. C., Vol. 5, Gordon and Breach, New York, 1970, pp. 405–426.

[22] Nazar, R., Amin, N., Filip, D., and Pop, I., "Stagnation Point Flow of a Micropolar Fluid Towards a Stretching Sheet," *International Journal of Non-Linear Mechanics*, Vol. 39, No. 7, 2004, pp. 1227–1235. doi:10.1016/j.ijnonlinmec.2003.08.007

[23] Ishak, A., Nazar, R., and Pop, I., "Mixed Convection on the Stagnation Point Flow Toward a Vertical, Continuously Stretching Sheet," *Journal of Heat Transfer*, Vol. 129, No. 8, 2007, pp. 1087–1090. doi:10.1115/1.2737482

[24] Ramadan, K., and Al-Nimr, M. A., "On Impulsively Started Convection: The Case of Stagnation Point Flow," *International Journal of Thermal Sciences*, Vol. 50, No. 12, 2011, pp. 2355–2364. doi:10.1016/j.ijthermalsci.2011.07.013

[25] Kogan, M. N., *Rarefied Gas Dynamics*, Plenum, New York, 1969, pp. 386–400.

[26] Kiwan, S., and Al-Nimr, M. A., "Flow and Heat Transfer Over a Stretched Microsurface," *Journal of Heat Transfer*, Vol. 131, No. 6, 2009, pp. 1–8. doi:10.1115/1.3090811

[27] Kiwan, S., and Al-Nimr, M. A., "Investigation into the Similarity Solution for Boundary Layer Flows in Microsystems," *Journal of Heat Transfer*, Vol. 132, No. 4, 2010, pp. 1–9. doi:10.1115/1.4000886

[28] Aziz, A., "Hydrodynamic and Thermal Slip Flow Boundary Layers Over a Flat Plate with Constant Heat Flux Boundary Condition," *Communications in Nonlinear Science and Numerical Simulation*, Vol. 15, No. 3, 2010, pp. 573–580. doi:10.1016/j.cnsns.2009.04.026

[29] Rahman, M. M., "Locally Similar Solutions for Hydromagnetic and Thermal Slip Flow Boundary Layers Over a Flat Plate with Variable Fluid Properties and Convective Surface Boundary Condition," *Meccanica*, Vol. 46, No. 5, 2011, pp. 1127–1143. doi:10.1007/s11012-010-9372-2

[30] Das, K., "Impact of Thermal Radiation on MHD Slip Flow Over a Flat Plate with Variable Fluid Properties," *Heat and Mass Transfer*, Vol. 48, No. 5, 2012, pp. 767–778. doi:10.1007/s00231-011-0924-3

[31] Martin, M. J., and Boyd, I. D., "Momentum and Heat Transfer in a Laminar Boundary Layer with Slip Flow," *Journal of Thermophysics and Heat Transfer*, Vol. 20, No. 4, 2006, pp. 710–719. doi:10.2514/1.22968

[32] Martin, M. J., and Boyd, I. D., "Falkner–Skan Flow Over a Wedge with Slip Boundary Conditions," *Journal of Thermophysics and Heat Transfer*, Vol. 24, No. 2, 2010, pp. 263–270. doi:10.2514/1.43316

[33] Chaudhary, R. C., and Jain, P., "Combined Heat and Mass Transfer in Magneto-Micropolar Fluid Flow from Radiate Surface with Variable Permeability in Slip-Flow Regime," *Zeitschrift für Angewandte Mathematik und Mechanik*, Vol. 87, Nos. 8–9, 2007, pp. 549–563. doi:10.1002/(ISSN)1521-4001

[34] Yazdi, M. H., Abdullah, S., Hashim, I., and Sopian, K., "Slip MHD Liquid Flow and Heat Transfer Over Non-Linear Permeable Stretching Surface with Chemical Reaction," *International Journal of Heat and Mass Transfer*, Vol. 54, Nos. 15–16, 2011, pp. 3214–3225. doi:10.1016/j.ijheatmasstransfer.2011.04.009

[35] Sahoo, B., "Flow and Heat Transfer of a Non-Newtonian Fluid Past a Stretching Sheet with Partial Slip," *Communications in Nonlinear Science and Numerical Simulation*, Vol. 15, No. 3, 2010, pp. 602–615. doi:10.1016/j.cnsns.2009.04.032

[36] Hayat, T., Javed, T., and Abbas, Z., "Slip Flow and Heat Transfer of a Second Grade Fluid Past a Stretching Sheet Through a Porous Space," *International Journal of Heat and Mass Transfer*, Vol. 51, Nos. 17–18, 2008, pp. 4528–4534. doi:10.1016/j.ijheatmasstransfer.2007.12.022

[37] Aziz, A., "A Similarity Solution for Laminar Thermal Boundary Layer Over a Flat Plate with a Convective Surface Boundary Condition," *Communications in Nonlinear Science and Numerical Simulation*, Vol. 14, No. 4, 2009, pp. 1064–1068. doi:10.1016/j.cnsns.2008.05.003

[38] Abraham, J. P., and Sparrow, E. M., "Friction Drag Resulting from the Simultaneous Imposed Motions of a Freestream and Its Bounding Surface," *International Journal of Heat and Fluid Flow*, Vol. 26, No. 2, 2005, pp. 289–295. doi:10.1016/j.ijheatfluidflow.2004.08.007

[39] Sparrow, E. M., and Abraham, J. P., "Universal Solutions for the Streamwise Variation of the Temperature of a Moving Sheet in the Presence of a Moving Fluid," *International Journal of Heat and Mass Transfer*, Vol. 48, No. 15, 2005, pp. 3047–3056. doi:10.1016/j.ijheatmasstransfer.2005.02.028

[40] Ishak, A., Yacob, N. A., and Bachok, N., "Radiation Effects on the Thermal Boundary Layer Flow Over a Moving Plate with Convective Boundary Condition," *Meccanica*, Vol. 46, No. 4, 2011, pp. 795–801. doi: 10.1007/s11012-010-9338-4

[41] Jafar, K., Ishak, A., and Nazar, R., "Magnetohydrodynamic Stagnation Point Flow with a Convective Surface Boundary Condition," *Zeitschrift für Naturforschung A*, Vol. 66, Nos. 8–9, 2011, pp. 495–499. doi:10.5560/ZNA.2011-0013

[42] Bataller, R. C., "Radiation Effects for the Blasius and Sakiadis Flows with a Convective Surface Boundary Condition," *Applied Mathematics*

and Computation, Vol. 206, No. 2, 2008, pp. 832–840.
doi:10.1016/j.amc.2008.10.001

[43] Makinde, O. D., and Aziz, A., "MHD Mixed Convection from a Vertical Plate Embedded in a Porous Medium with a Convective Boundary Condition," *International Journal of Thermal Sciences*, Vol. 49, No. 9, 2010, pp. 1813–1820.
doi:10.1016/j.ijthermalsci.2010.05.015

[44] Yao, S., Fang, T., and Zhong, Y., "Heat Transfer of a Generalized Stretching/Shrinking Wall Problem with Convective Boundary Conditions," *Communications in Nonlinear Science and Numerical Simulation*, Vol. 16, No. 2, 2011, pp. 752–760.
doi:10.1016/j.cnsns.2010.05.028

[45] Ishak, A., Nazar, R., and Pop, I., "Magnetohydrodynamic (MHD) Flow of a Micropolar Fluid Towards a Stagnation Point on a Vertical Surface," *Computers & Mathematics with Applications*, Vol. 56, No. 12, 2008, pp. 3188–3194.
doi:10.1016/j.camwa.2008.09.013

[46] Hayat, T., Hussain, M., Hendi, A. A., and Nadeem, S., "MHD Stagnation Point Flow Towards Heated Shrinking Surface Subjected to Heat Generation/Absorption," *Applied Mathematics and Mechanics*, Vol. 33, No. 5, 2012, pp. 631–648.
doi:10.1007/s10483-012-1576-6

[47] Ahmedi, G., "Self-Similar Solution of Incompressible Micropolar Boundary Layer Flow Over a Semi-Infinite Plate," *International Journal of Engineering Science*, Vol. 14, No. 7, 1976, pp. 639–646.
doi:10.1016/0020-7225(76)90006-9

[48] Jena, S. K., and Mathur, M. N., "Similarity Solutions for Laminar Free Convection Flow of a Thermomicropolar Fluid Past a Non-Isothermal Vertical Flat Plate," *International Journal of Engineering Science*, Vol. 19, No. 11, 1981, pp. 1431–1439.
doi:10.1016/0020-7225(81)90040-9

[49] El-Gendi, S. E., "Chebyshev Solution of Differential, Integral and Integro-Differential Equations," *Computer Journal*, Vol. 12, No. 3, 1969, pp. 282–287.
doi:10.1093/comjnl/12.3.282

[50] Boutros, Z. Y., Abd-el-Malek, M. B., Badran, N. A., and Hassan, S. H., "Lie-Group Method of Solution for Steady Two-Dimensional Boundary-Layer Stagnation-Point Flow Towards a Heated Stretching Sheet Placed in a Porous Medium," *Meccanica*, Vol. 41, No. 6, 2006, pp. 681–691.
doi:10.1007/s11012-006-9014-x

[51] Pop, S. R., Grosan, T., and Pop, I., "Radiation Effects on the Flow Near the Stagnation Point of a Stretching Sheet," *Technische Mechanik*, Vol. 25, No. 2, 2004, pp. 100–106.